

Deep HI observations* of the surroundings of ram pressure stripped Virgo spiral galaxies

Where is the stripped gas?

B. Vollmer¹ & W. Huchtmeier²

¹ CDS, Observatoire astronomique de Strasbourg, UMR 7550, 11, rue de l'université, 67000 Strasbourg, France

² Max-Planck-Institut für Radioastronomie, Auf dem Hügel 69, 53121 Bonn Germany

Received / Accepted

Abstract. Deep Effelsberg 100-m HI observations of 5 HI deficient Virgo spiral galaxies are presented. No new extended HI tail is found in these galaxies. The already known HI tail north of NGC 4388 does not significantly extend further than a WSRT image has shown. Based on the absence of HI tails in a sample of 6 Virgo spiral galaxies and a balance of previous detections of extraplanar gas in the targeted galaxies we propose a global picture where the outer gas disk (beyond the optical radius R_{25}) is removed much earlier than expected by the classical ram pressure criterion. Based on the two-phase nature of atomic hydrogen located in a galactic disk, we argue that the warm diffuse HI in the outer galactic disk is evaporated much more rapidly than the cold dense HI. Therefore, after a ram pressure stripping event we can only observe atomic hydrogen which was cold and dense before it was removed from the galactic disk. This global picture is consistent with all available observations. We detect between 0.3% and 20% of the stripped mass assuming an initially non-deficient galaxy and between 3% and 70% of the stripped mass assuming an initially HI deficient galaxy ($\text{def}=0.4$). Under the latter assumption we estimate an evaporation rate by dividing the missing mass by the estimated time to peak ram pressure from dynamical simulations. We find evaporation rates between 10 and 100 $M_{\odot}\text{yr}^{-1}$.

Key words. Galaxies: individual: NGC 4388, NGC 4402, NGC 4438, NGC 4501, NGC 4522 – Galaxies: interactions – Galaxies: ISM – Galaxies: kinematics and dynamics

1. Introduction

The HI properties of cluster spiral galaxies are significantly different from those of field spiral galaxies. Spiral galaxies located near the cluster center are often HI deficient (Chamaraux et al. 1980, Bothun et al. 1982, Giovanelli & Haynes 1985, Gavazzi 1987, 1989) and their HI disk sizes are considerably reduced (van Gorkom & Kotanyi 1985, Warmels 1988, Cayatte et al. 1990, 1994). The observed small HI disks together with unperturbed old stellar disks favor a ram pressure stripping scenario as the origin of the HI deficiency of Virgo cluster spirals. Fourteen out of the 22 brightest Virgo spiral galaxies show an HI deficiency greater than 0.3 (Cayatte et al. 1994), i.e. they have lost more than half of their initial reservoir of atomic hydrogen. This represents more than $10^9 M_{\odot}$ per galaxy. Despite the large missing mass, it is very difficult to ob-

serve this stripped gas. In the Virgo cluster an extended gas tail is only observed in one spiral galaxy.

This exception is NGC 4388 which is located at a projected distance of 1.3° ($\sim 0.4 \text{ Mpc}^1$) from the Virgo cluster center (M87) and hosts a Seyfert 2 nucleus. Yoshida et al. (2002) discovered a very large $\text{H}\alpha$ plume that extends up to $\sim 35 \text{ kpc}$ north eastwards from the galactic disk which is seen almost edge-on. This region contains $\sim 10^5 M_{\odot}$ of ionized gas. Vollmer & Huchtmeier (2003) were the first who detected atomic hydrogen associated with this plume. Oosterloo & van Gorkom (2005) imaged this gas tail with the WSRT and found an extent of $\sim 100 \text{ kpc}$ and a mass of $3.4 \times 10^8 M_{\odot}$. This represents only about 20% of the stripped gas assuming an HI deficiency of 0.8 (Cayatte et al. 1994).

These arguments only hold if the spiral galaxy had as much gas as a field galaxy of the same optical diameter and the same morphology before the ram pressure stripping event. On the other hand, cluster galaxies might have experienced other gas removing interactions before

Send offprint requests to: B. Vollmer, e-mail: bvollmer@astro.u-strasbg.fr

* Based on 100-m Effelsberg radio telescope observations

¹ We use a distance of 17 Mpc to the Virgo cluster

ram pressure stripping. Possible interactions can be divided into two classes (for a review see Gavazzi & Boselli 2006): (i) the “preprocessing” of spiral galaxies through tidal interactions in infalling galaxy groups (Mihos 2004, Fujita 2004, Dressler 2004) and (ii) harassment (Moore et al. 1996, 1998), viscous/turbulent stripping (Nulsen 1982) and/or thermal evaporation (Cowie & McKee 1977) which occur once the galaxy resides within the cluster. These mechanisms make the missing mass decreasing but not vanish. We still expect several $10^8 M_{\odot}$ of stripped gas which is not detected.

The question thus arises where the stripped gas is hidden and if we can or should detect it. The underlying problem is the evolution of the multiphase ISM once it is pushed out of the galactic disk by ram pressure. Within the starforming disk the ISM is turbulent and consists of several phases: the hot ionized ($\sim 10^6$ K), the warm neutral and ionized ($\sim 10^4$ K), and the cold neutral (~ 100 K) phase (see, e.g. Kulkarni & Heiles 1988, Spitzer 1990, McKee 1995). The neutral phase is not uniform but of fractal nature (Elmegreen & Falgarone 1996). Braun (1997) analyzed the resolved neutral hydrogen emission properties of the 11 nearest spiral galaxies. He identified the high-brightness network of HI emission features with the cold neutral medium ($T \sim 100$ K) and found that the bulk of atomic hydrogen is in this cold phase (between 60% and 90%). Braun (1997) also noted that the fractional line flux due to the cold phase drops abruptly near the optical radius of a given galaxy. However, beyond this radius a cool phase still exists in most of the galaxies, even though it represents only a few percent of the total HI flux.

When the ISM is leaving the disk, its heating (kinematical heating by supernova explosions and heating by stellar radiation) decreases and the whole gas is surrounded by the hot intracluster medium (ICM). At the same time ram pressure driven shocks propagate through the ISM. Initially dense ISM regions might collapse and form stable globules (Vollmer et al. 2001) or form stars, whereas tenuous regions might expand. The intracluster medium does not only confine the stripped gas, but also causes evaporation (Cowie & McKee 1977). How efficient evaporation is depends on the geometry of the magnetic field frozen into the ISM. A tangled field will increase the evaporation timescale considerably (Cowie et al. 1981, Malyskin & Kulsrud 2001). Since the magnetic field geometry is not accessible, only direct observations of the stripped gas at different wavelengths can help us to determine what happens to the ISM once it has left the galactic disk.

In this article we approach this problem with deep single dish HI observations to search for atomic hydrogen far away from the galactic disks (> 20 kpc) and a balance of previous detections of extraplanar gas. We selected 5 galaxies for which deep interferometric HI observations showed extraplanar gas. The observations are described in Sect. 2 followed by the presentation of the results (Sect. 3). These results are discussed in the framework of the stripping of a two-phase atomic hydrogen taking into account

Table 1. Integration times and rms.

NGC 4402						
position	C	NW	W	SW	SE	NE
Δt (min)	120	120	–	120	120	120
rms (mJy)	2.6	1.8	–	2.0	1.5	3.5
NGC 4438						
position	C	NW	W	SW	SE	NE
Δt (min)	120	120	120	120	120	120
rms (mJy)	1.8	1.7	1.8	2.2	2.2	2.2
NGC 4501						
position	C	NW	W	SW	SE	NE
Δt (min)	120	120	–	120	120	120
rms (mJy)	1.8	1.0	–	1.4	1.6	1.7
NGC 4522						
position	C	NW	W	SW	SE	NE
Δt (min)	120	120	–	120	120	120
rms (mJy)	1.2	1.8	–	1.9	1.1	1.2

existing detections of extraplanar gas (Sect. 4). Finally, we give our conclusions in Sect. 5.

2. Observations

In 2001–2003, we performed 21-cm line observations with the Effelsberg 100-m telescope at different positions centered on the systemic velocities of NGC 4402, NGC 4438, NGC 4501, and NGC 4522 with a bandwidth of 12.5 MHz. The two-channel receiver had a system noise of ~ 30 K. The 1024 channel autocorrelator was split into four banks with 256 channels each, yielding a channel separation of ~ 10 km s^{-1} . We further binned the channels to obtain a final channel separation of ~ 10 km s^{-1} like the archival VLA data which we use for comparison (NGC 4402, NGC 4501, NGC 4522). The galaxy’s central position and four positions at a distance of one beam width (9.3′) to the NW, SW, SE, and NE from the galaxy center were observed in on–off mode (5 min on source, 5 min off source). In addition, we observed a sixth position 6.5′ west of the galaxy center for NGC 4438. Care was taken to avoid other Virgo cluster galaxies with velocities within our bandwidth in all observations. We used 3C286 for pointing and flux calibration. The observation time was 120 min per position. The resulting noise (Table 1) is partly determined by small amplitude interferences, but it is close to the theoretical noise of 2 mJy per hour of integration: on average $1\sigma = 1.5$ mJy (varying from 1.1 to 2.0 mJy).

In addition we observed a field of about $1^{\circ} \times 1^{\circ}$ centered on the HI plume of NGC 4388. The noise level of

these spectra is largely determined by the closeness of M87 which has a flux density of ~ 220 Jy at 1.4 GHz. The noise of our spectra varies between $1\sigma = 2$ and 7 mJy.

In order to compare our Effelsberg HI spectra to interferometric data where the galaxy is spatially resolved, we use VLA 21 cm data (Crowl et al. 2005, Vollmer et al. in prep., Kenney et al. 2004). These data have spatial resolutions of $\sim 20''$ and channel separations of 10 km s^{-1} . We clipped the data cubes at a level of 3 mJy/beam and produced a synthesized single dish spectrum using a Gaussian beam of $9.3'$ HPBW.

3. Results

3.1. NGC 4388

We observed 6×5 positions centered on the HI plume of NGC 4388 (Oosterloo & van Gorkom 2005) (Fig. 1). The spectrum centered on NGC 4388 is labeled with a ‘‘G’’. The observing conditions did not permit us to obtain interference-free spectra of two positions in the north-east of NGC 4388. In the corresponding boxes we have replaced the spectra by a solid line. The sinusoidal behaviour of the spectra in the west and the east is most probably due to sidelobe detection of M87. We clearly detect HI line emission in 4 positions: in NGC 4388 and in 3 positions to the north west of the galactic disk. These positions are labeled with ‘‘tail’’. One of the spectra shows a double line profile consistent with the WSRT observations of Oosterloo & van Gorkom (2005). Our deep HI observations show that there is no significant amount of atomic hydrogen beyond this HI tail.

3.2. NGC 4402

NGC 4402 is another HI deficient edge-on spiral located close to NGC 4388. Crowl et al. (2005) detected an asymmetric distribution of the 20cm continuum emission and $2.7 \times 10^7 M_{\odot}$ of extraplanar atomic hydrogen in the north east of the galactic disk. Both features are consistent with a scenario where ram pressure is responsible for the compressed radio continuum halo and the extraplanar HI. Our Effelsberg observations of the central position Fig. 2 do not reveal more HI than observed with the VLA (Crowl et al. 2005). We do not find any HI in the offset positions (Fig. 3). The gap in the spectrum around zero radial velocity is due to galactic HI emission.

3.3. NGC 4438

NGC 4438 has a strongly perturbed stellar disk with a prominent stellar tidal arm pointing to the north. This perturbation is due to a rapid and close gravitational interaction with its companion S0 galaxy NGC 4435 (Combes et al. 1988, Vollmer et al. 2005). The gas disk is heavily truncated and almost exclusively molecular. Extraplanar CO with a mass of $\sim 5 \times 10^8 M_{\odot}$ is detected to the west of the galactic disk. Detailed modelling of the interaction

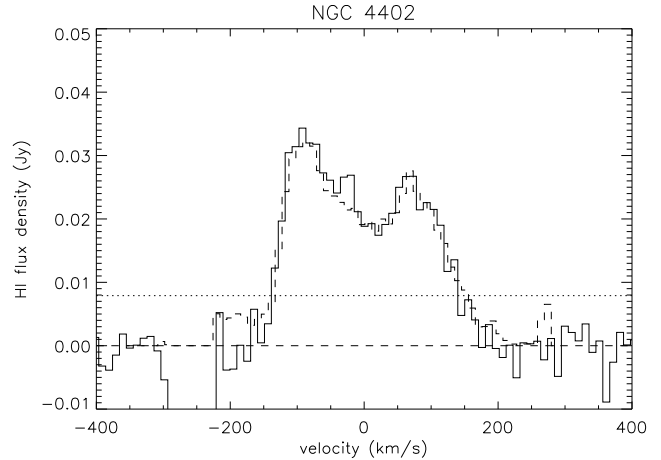


Fig. 2. Solid line: Effelsberg 100-m spectrum of the central position. Dashed line: spectrum of the VLA data (Crowl et al. 2005). Dotted line: 3σ noise level of the 100-m spectrum. Heliocentric velocities are given relative to the systemic velocity of NGC 4402 ($v_{\text{sys}}=235 \text{ km s}^{-1}$).

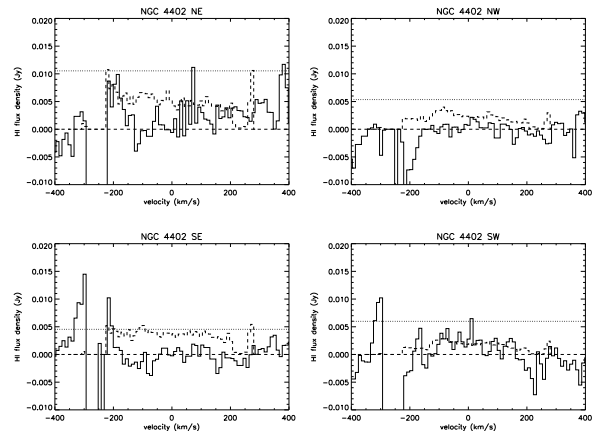


Fig. 3. Solid lines: Effelsberg 100-m spectra of the four off-center positions. Their locations with respect to the galaxy center are marked on top of each panel. Dashed line: synthesized VLA spectra (Crowl et al. 2005), which only show HI disk emission. Dotted line: 3σ noise levels of the Effelsberg spectra. Radial velocities are given relative to the systemic velocity of NGC 4402.

including the gravitational interaction, ram pressure, and an ISM-ISM collision showed that ram pressure (together with the tidal interaction) is the most important ingredient to reproduce the observed CO emission distribution and kinematics (Vollmer et al. 2005).

With our deep Effelsberg observations, linearly interpolated where galactic HI emission dominates, we detect a total HI mass of $\sim 6 \times 10^8 M_{\odot}$ (Fig. 4). Since there is only a small fraction of the total HI emission detected in interferometric radio observations (Cayatte et al. 1990, Hibbard et al. 2001), we compare our deep Effelsberg HI

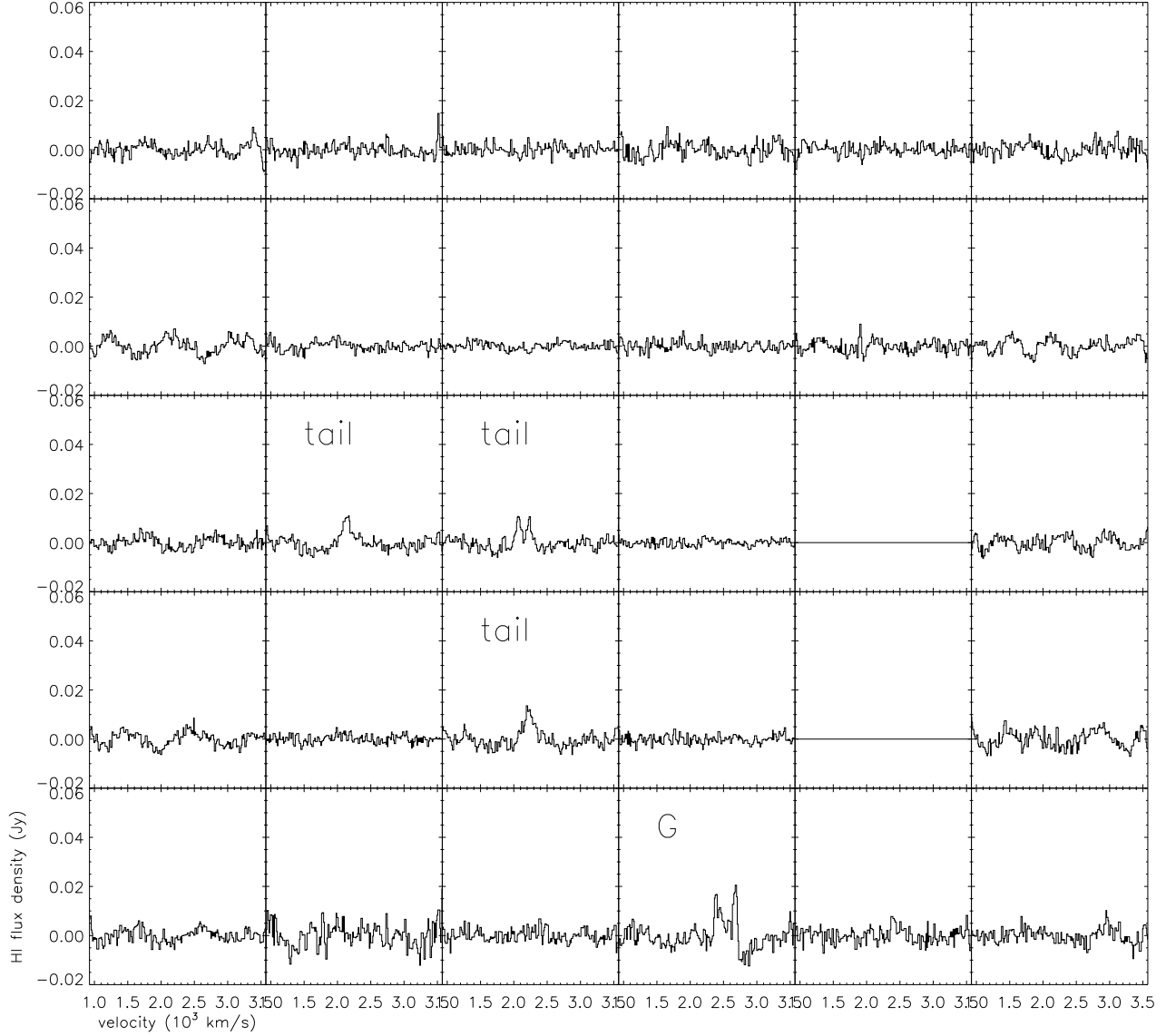


Fig. 1. Deep Effelsberg 100-m HI spectra of the NGC 4388 HI plume. The spectrum centered on the galaxy is labeled with a “G”. We clearly detect HI line emission in 4 positions: in NGC 4388 and in 3 positions to the north west of the galactic disk. These positions are labeled with “tail”. The spatial separation between two spectra corresponds to the beamsize (9.3’). We were not able to obtain proper spectra for two positions north west of the galaxy. In the corresponding boxes we have replaced the spectra by a solid line.

spectrum with the integrated CO spectrum of Vollmer et al. (2005) where the extraplanar gas is included. We find a remarkable resemblance between the two spectra tracing the molecular and the atomic hydrogen. The only differences are that (i) the ratio between the HI peak flux density at $v = 0 \text{ km s}^{-1}$ and $v > 0 \text{ km s}^{-1}$ is larger than that of the CO data and (ii) the CO peak at $v > 0 \text{ km s}^{-1}$ extends further to high velocities. This might indicate that both gas phases are well mixed. However, without deep interferometric HI observations, which are still lacking due to the closeness of M87, it is not possible to investigate the HI – H₂ connection in more detail. We do not find any

significant HI in the offset positions (Fig. 5).

3.4. NGC 4501

The spiral galaxy NGC 4501 has an HI disk which is truncated close to the optical radius R_{25} . In addition, the HI surface density is enhanced in the south western side of the galactic disk (Cayatte et al. 1990, 1994). In a forthcoming paper (Vollmer et al., in prep.) we will show that this galaxy is in a pre-peak stripping stage, i.e. it is approaching the cluster center and ram pressure will reach its maximum in about 100 Myr. Our deep Effelsberg HI

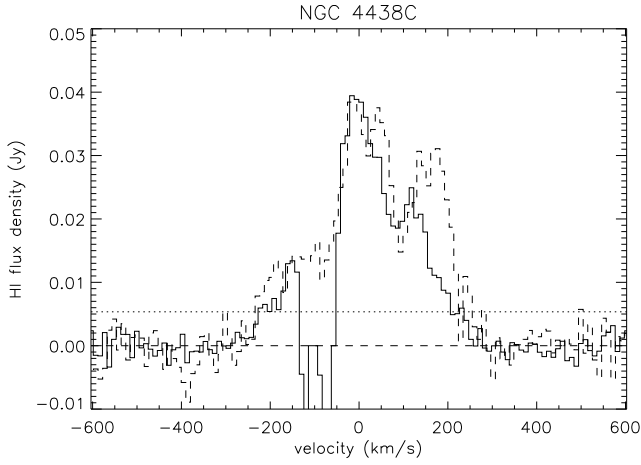


Fig. 4. Solid line: Effelsberg 100-m spectrum of the central position. Dashed line: CO(1–0) spectrum from Vollmer et al. (2005) in arbitrary units. Dotted line: 3σ noise level of the 100-m spectrum. Heliocentric velocities are given relative to the systemic velocity of NGC 4438 ($v_{\text{sys}} = 70 \text{ km s}^{-1}$).

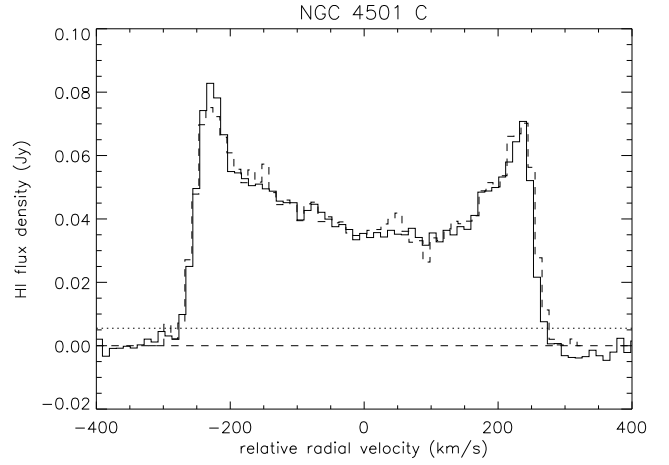


Fig. 6. Solid line: Effelsberg 100-m spectrum of the central position. Dashed line: spectrum of the VLA data (Vollmer et al. in prep.). Dotted line: 3σ noise level of the 100-m spectrum. Heliocentric velocities are given relative to the systemic velocity of NGC 4501 ($v_{\text{sys}} = 2281 \text{ km s}^{-1}$).

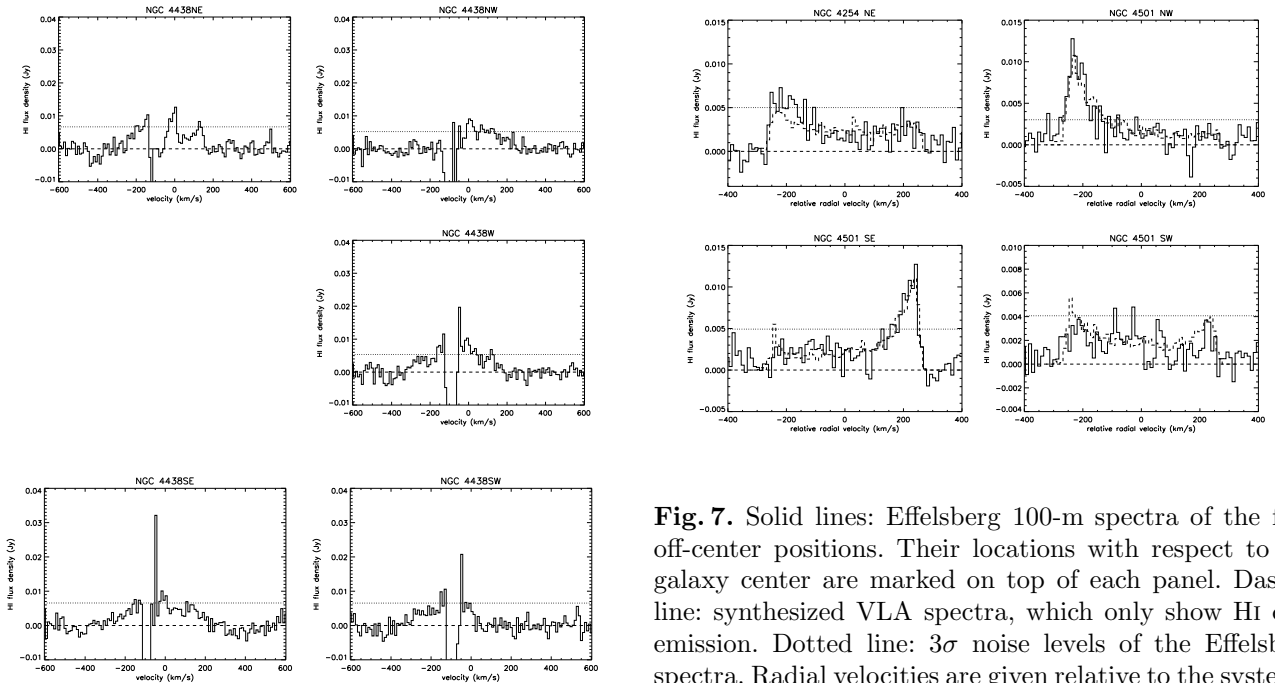


Fig. 5. Solid lines: Effelsberg 100-m spectra of the five off-center positions. Their locations with respect to the galaxy center are marked on top of each panel. Dotted line: 3σ noise levels of the Effelsberg spectra. Radial velocities are given relative to the systemic velocity of NGC 4438.

observations of the central position (Fig. 6) do not reveal more HI than observed with the VLA (Vollmer et al., in prep.). The single dish Effelsberg spectra of the offset positions show a possible additional HI flux density compared to the VLA data in the north-east of the galactic disk (Fig. 7). This extra emission corresponds to an HI mass of

Fig. 7. Solid lines: Effelsberg 100-m spectra of the four off-center positions. Their locations with respect to the galaxy center are marked on top of each panel. Dashed line: synthesized VLA spectra, which only show HI disk emission. Dotted line: 3σ noise levels of the Effelsberg spectra. Radial velocities are given relative to the systemic velocity of NGC 4501.

$\sim 10^7 M_{\odot}$. This is consistent with the pre-peak stripping scenario.

3.5. NGC 4522

NGC 4522 is one of the best examples for ongoing ram pressure stripping. HI and H α observations (Kenney et al. 2004, Kenney & Koopmann 1999) showed a heavily truncated gas disk at a radius of 3 kpc, which is $\sim 40\%$ of the optical radius, and a significant amount of extraplanar gas to the west of the galactic disk ($1.5 \times 10^8 M_{\odot}$). The

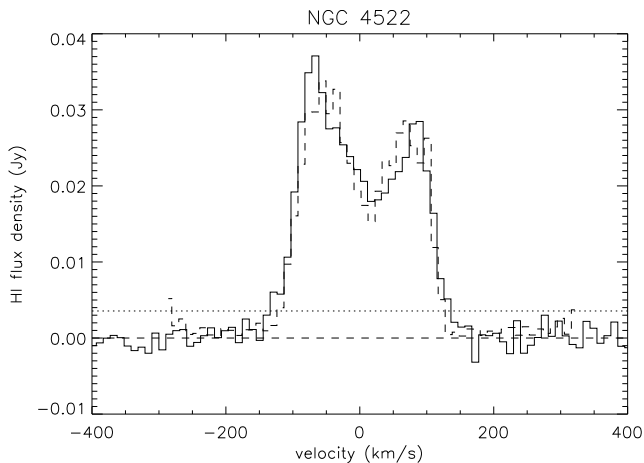


Fig. 8. Solid line: Effelsberg 100-m spectrum of the central position. Dashed line: spectrum of the VLA data of Kenney et al. (2004). Dotted line: 3σ noise level of the 100-m spectrum. Heliocentric velocities are given relative to the systemic velocity of NGC 4522 ($v_{\text{sys}}=2324 \text{ km s}^{-1}$).

one-sided extraplanar atomic gas distribution shows high column densities, comparable to those of the adjacent galactic disk. A strong ram pressure scenario can account for the truncated gas disk and the western extraplanar gas. Further evidence for such a peak ram pressure scenario comes from polarized radio continuum observations (Vollmer et al. 2004b). The 6 cm polarized emission is located at the eastern edge of the galactic disk, opposite to the western extraplanar gas. This ridge of polarized radio continuum emission is most likely due to ram pressure compression of the interstellar medium (ISM) and its magnetic field. In addition, the degree of polarization decreases from the east to the west and the flattest spectral index between 20 cm and 6 cm coincides with the peak of the 6 cm polarized emission. These findings together with a detailed dynamical model (Vollmer et al. 2006) are consistent with a scenario where ram pressure is close to its maximum. Our Effelsberg observations of the central position (Fig. 8) do not reveal more HI than observed with the VLA (Kenney et al. 2004). We do not find any HI in the offset positions (Fig. 9).

3.6. NGC 4569

Deep VLA and Effelsberg HI data together with a dynamical model of this galaxy are presented in Vollmer et al. (2004a). They discovered a low surface density HI arm in the west of the galaxy, whose velocity field is distinct from that of the overall disk rotation. No HI emission was detected in the Effelsberg HI off center observations. A post-stripping scenario is consistent with the main observed characteristics of NGC 4569. In this scenario the galaxy’s closest approach to the cluster center, i.e. peak ram pressure, occurred $\sim 300 \text{ Myr}$ ago.

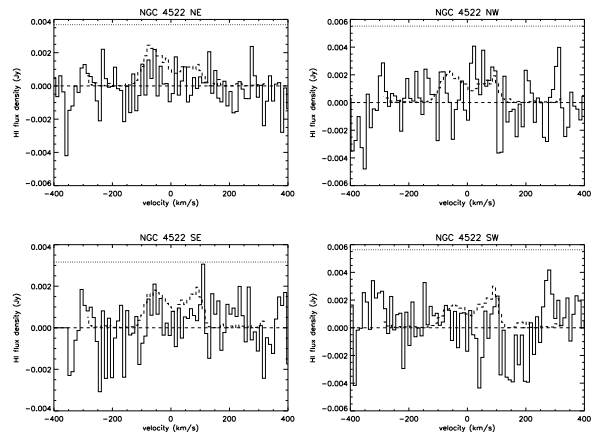


Fig. 9. Solid lines: Effelsberg 100-m spectra of the four off-center positions. Their locations with respect to the galaxy center are marked on top of each panel. Dashed line: synthesized VLA spectra (Kenney et al. 2004), which only show HI disk emission. Dotted line: 3σ noise levels of the Effelsberg spectra. Radial velocities are given relative to the systemic velocity of NGC 4522.

4. Where did the ram pressure stripped gas go?

With our sample of 6 galaxies we can now investigate how much of the missing stripped gas mass we detect in HI. The first result is that we do not detect a significant amount of atomic hydrogen at distances greater than 20 kpc in any of these galaxies except in NGC 4388 (see Sec. 4.5). For the determination of a gas detection rate we need to know the expected atomic gas mass of a non-HI deficient galaxy. With the HI deficiency and the total observed HI mass we can estimate the expected initial HI mass of a spiral galaxy before it entered the Virgo cluster (table 2). As discussed in Sec. 1 this depends on whether the galaxy experienced a gas removing interaction before the ram pressure stripping event. Therefore we calculate the initial HI mass for a “normal” field galaxy and a galaxy that has already lost a significant amount of gas due to tidal interactions, turbulent/viscous stripping, and/or evaporation.

4.1. Initially “normal” gas rich spiral galaxies

In general, the uncertainty of HI deficiencies is about ± 0.2 . We use the HI deficiencies of Crowl et al. (2005) and Kenney et al. (2004) which are consistent with those of Cayatte et al. (1994) within the errors. If we assume that the missing (non-detected) gas has been evaporated by the hot intracluster medium, we can estimate the evaporation rate by dividing the missing mass by a characteristic timescale. For this timescale we chose the time to ram pressure peak when most of the gas leaves the galaxy. Detailed comparison between observations and numerical modelling of these galaxies showed that we observe NGC 4388 $\sim 100 \text{ Myr}$ after peak ram pressure (Vollmer &

Huchtmeier 2003), NGC 4402 more than several 100 Myr after peak ram pressure (Crowl et al. 2005), NGC 4438 is near peak ram pressure (Vollmer et al. 2005), NGC 4501 is ~ 100 Myr before peak ram pressure (Vollmer et al. in prep.), NGC 4522 is near peak ram pressure (Vollmer et al. 2006), and NGC 4569 ~ 300 Myr after peak ram pressure (Vollmer et al. 2004a).

Table 2 summarizes the data for all galaxies: the time to peak ram pressure (col.(2)), the HI deficiency (col.(3)), the observed total HI mass (col(4)), the observed extraplanar HI gas mass (col.(5); except for NGC 4438 where we have taken the extraplanar CO mass), the expected HI mass based on the HI deficiency (col.(6)), the percentage of extraplanar gas to the missing gas mass, i.e. the difference between the observed and the expected initial gas mass (col.(7)), the expected HI mass assuming an initial HI deficiency of 0.4 (col.(8)), the percentage of extraplanar gas to the missing gas mass assuming an initial HI deficiency of 0.4 (col.(9)), and the estimated evaporation rate (1; col.(10)).

The percentage of extraplanar gas mass with respect to the expected gas mass assuming an initially non-HI deficient galaxy varies between 0.3% and 20%. Thus, more than 80% of the missing gas is undetectable in HI.

4.2. Initially gas deficient spiral galaxies

The assumption of an initially non-HI deficient galaxy is however questionable. We argue that the interplay between ram pressure and evaporation of the galaxy’s ISM by the hot intracluster medium might be different between (i) the inner gas disk where star formation occurs and the gas is clumpy and multiphase and (ii) the outer gas disk where the atomic hydrogen is mainly warm ($T \sim 10^4$ K) and smoothly distributed (see e.g. Braun 1997). In the inner star forming disk ($R < R_{25}$) the gas is turbulent and clumpy giving rise to a tangled magnetic field which suppresses evaporation (Cowie et al. 1981, Malyskin & Kulsrud 2001). On the other hand, due to the kinematical quietness and the smoothness of the outer gas disk, the magnetic field there is expected to be less tangled leading to a much more efficient evaporation of the warm HI. Because of this effect together with the fact that the gas surface density decreases with increasing galactic radius in the outer gas disk, the outer gas is much more vulnerable to evaporation, harassment, turbulent/viscous stripping and ram pressure. We therefore argue that the outer gas disk is stripped and evaporated at much larger distances from the cluster center than one would expect from the Gunn & Gott criterion (Gunn & Gott 1972). However, an early gas removal by “preprocessing” is also possible.

Based on this argument, we can recalculate the expected initial gas mass assuming that the gas disk is truncated at the optical radius (R_{25}). Spiral galaxies which show this property in the Cayatte et al. (1994) sample have a mean HI deficiency of 0.4. We thus recalculated the expected atomic gas mass assuming this initial HI de-

ciency (Table 2 col.(8)) and the percentage of extraplanar gas mass with respect to the expected gas mass (Table 2 col.(9)). These percentage lie between 3% and 70%. The galaxies that we observe close or up to 100 Myr after peak ram pressure still have about half of the stripped gas in neutral form.

As a final step we can estimate an evaporation rate by

$$\dot{M}_{\text{evap}} \sim (M_{\text{HI}}^{\text{def}=0.4} - M_{\text{HI}}^{\text{total}})/t_{\text{rps}}, \quad (1)$$

where $M_{\text{HI}}^{\text{def}=0.4}$ is the expected HI mass assuming an initial HI deficiency of 0.4, $M_{\text{gas}}^{\text{total}}$ is the observed total HI mass (from table 2), and t_{rps} is the time to peak ram pressure. This evaporation rate can be found in Table 2 col.(10). We took here the time to peak ram pressure as the characteristic timescale. Because it is not possible to determine if evaporation happened faster, this timescale is an upper limit and, consequently, the derived evaporation rate represents a lower limit.

4.3. Evaporation rates

Since NGC 4501 is in a pre-peak ram pressure phase, we cannot estimate an evaporation timescale. It is intriguing that the three galaxies which are only affected by ram pressure and which are observed less than 400 Myr after peak ram pressure show the same evaporation rate of about $\dot{M}_{\text{evap}} \sim 5 - 11 \text{ M}_{\odot}\text{yr}^{-1}$. The case of NGC 4438 is complicated, because of the unknown HI deficiency, the additional tidal and ISM-ISM interactions, and a possible phase transition of the displaced gas, but since ram pressure has the greatest effect on its ISM the derived evaporation rate might still be valuable.

The analytical estimate of the classical evaporation rate of a spherical gas cloud by Cowie & McKee (1977) is

$$\dot{M}_{\text{evap}} = 4.34 \times 10^{-22} T_{\text{ICM}}^{\frac{5}{2}} R_{\text{pc}} (30/\ln \Lambda) \text{ M}_{\odot}\text{yr}^{-1}. \quad (2)$$

For a cloud size of the order of the disk height $R_{\text{pc}} = 500$ pc, an ICM temperature of $T_{\text{ICM}} = 3 \times 10^7$ K, and a Coulomb logarithm of $\ln \Lambda = 30$, one finds $\dot{M}_{\text{evap}} \sim 1 \text{ M}_{\odot}\text{yr}^{-1}$. About 1000 clouds are necessary to fill an HI disk of constant height $H = 500$ pc between $R = 5$ kpc and $R = 10$ kpc. If these clouds have a density of $n = 1 \text{ cm}^{-3}$ the resulting gas mass is about $1.5 \times 10^9 \text{ M}_{\odot}$. If 10% of the surface of these clouds are surrounded by the hot intracluster medium (this depends on the tail geometry) the resulting total evaporation rate is $\dot{M}_{\text{evap}}^{\text{tot}} \sim 100 \text{ M}_{\odot}\text{yr}^{-1}$.

Our derived evaporation rate of NGC 4438 is close to that value. This might imply that the evaporation timescale is short (of the order of 10 Myr). If we assume this short timescale for NGC 4388 and NGC 4522 we obtain evaporation rate of $56 \text{ M}_{\odot}\text{yr}^{-1}$ and $25 \text{ M}_{\odot}\text{yr}^{-1}$ which are close to the analytical estimate.

4.4. Amount of detected stripped gas

The percentage of the observed gas mass varies between 23% and 68% of the expected gas mass assuming an initial

Table 2. Galaxy gas properties.

name	time to ram pressure max. (Myr)	HI def	$M_{\text{HI}}^{\text{extra}}$ ($10^8 M_{\odot}$)	$M_{\text{HI}}^{\text{total}}$ ($10^8 M_{\odot}$)	$M_{\text{HI}}^{\text{expected}}$ ($10^8 M_{\odot}$)	% of missing mass	$M_{\text{HI}}^{\text{expected}}$ def = 0.4 ($10^8 M_{\odot}$)	% of missing mass	evaporation rate M_{\odot}/yr
NGC 4388	100 ^a	0.8 ^a	3.4 ^b	3.6 ^a	23	18	9.2	61	5.6
NGC 4402	> 300 ^a	0.5 ^c	0.3 ^c	4.4 ^c	14	3	5.6	23	< 0.4
NGC 4438	10 ^j	0.9 ^d	5.0 ^e	6.0 ^f	48	12	19	38	130
NGC 4501	-100 ^k	0.5 ^a	< 0.1 ^j	17 ^a	54	< 0.3	21	3	–
NGC 4522	50 ^l	0.6 ^g	1.7 ^g	4.3 ^g	17	14	6.8	68	5.0
NGC 4569	300 ^m	1.2 ^a	0.5 ^m	6.0 ^m	95	0.6	38	1.6	10.7

^a Cayatte et al. (1994)^b Oosterloo & van Gorkom (2005)^c Crowl et al. (2005)^d We took the HI deficiency of NGC 4579 which has about the same B and H band magnitudes and morphological type. As NGC 4438, it also shows a highly truncated gas disk with a very small amount of HI.^e CO gas mass from Vollmer et al. (2006)^f from this paper^g Kenney et al. (2004)^h Vollmer & Huchtmeier (2003)ⁱ Based on the low mass and low surface brightness extraplanar HI.^j Vollmer et al. (2005)^k Vollmer et al., in prep.^l Vollmer et al. (2006)^m Vollmer et al. (2004a)

HI deficiency of 0.4 for the galaxies which are stripped inside the optical radius (table 2 col.(9)). We argue that this corresponds to the fraction of cold HI in the galactic disk before it was stripped. This is entirely consistent with the results based on the deep HI observations of nearby undisturbed gas disks reported in (Braun 1997; see Sec. 1). We propose a scenario where the diffuse warm ($T \sim 8000$ K) HI evaporates rapidly and the cold ($T \sim 100$ K) HI resists much longer and can still be observed 100 Myr after its removal from the galactic disk. This scenario is also consistent with the HI observations and simulations of NGC 4522 (Kenney et al. 2004, Vollmer et al. 2006) where a low surface brightness HI component is detected with a large linewidth ($\sim 100 \text{ km s}^{-1}$). Vollmer et al. (2006) interpreted this component as diffuse warm HI which is stripped more efficiently than the cold dense HI. Here we add the effect of evaporation to this picture which might be partly responsible for the increased stripping efficiency.

4.5. The exception: NGC 4388

NGC 4388 is the only galaxy where extraplanar low surface density gas is detected at distances larger than 10 kpc from the galactic disk. Oosterloo & van Gorkom (2005) speculated that the HI tail did not evaporate, because NGC 4388 was stripped by the ICM of M86. This ICM is less dense and maybe cooler than that of the Virgo cluster, i.e. M87, and therefore evaporation is slower. However, M86 has a negative absolute velocity and lies far behind M87 (more than 1 Mpc, see, e.g., Vollmer et al. 2004c).

On the other hand, NGC 4388 is located close to M87 ($D \sim 2000 \text{ km s}^{-1} \times 100 \text{ Myr} \sim 0.1 \text{ Mpc}$). The deprojected tail length in a putative M86 stripping scenario would be $\sim 1 \text{ Mpc}$ which requires an unreasonable large evaporation time. The most forward explanation, which is consistent with our findings, is that NGC 4388 is the only galaxy that we are observing in an evolutionary stage long enough after peak ram pressure to show an extended gas tail and short enough after peak ram pressure so that the tail is not yet evaporated. This time window has a width of $\sim 200 \text{ Myr}$ compared to a cluster crossing time of $\sim 3 \text{ Gyr}$ explaining the low probability to observe a galaxy in this evolutionary stage.

5. Conclusions

We made deep HI observations with the Effelsberg 100-m telescope around 5 HI deficient Virgo spiral galaxies to search for neutral gas located far away from the galactic disks (more than 20 kpc). These galaxies are or were all affected by ram pressure stripping. The following results were obtained

- we did not detect HI emission far away from NGC 4402, NGC 4438, NGC 4501, and NGC 4522;
- the already known HI tail in the north of NGC 4388 does not extend further than the WSRT image of Oosterloo & van Gorkom (2005) has shown;
- the HI tail of NGC 4388 seems thus to be an exception.

Based on the absence of HI tails in these galaxies and a balance of previous detections of extraplanar gas in the

targeted galaxies we propose a global picture where the outer gas disk (beyond the optical radius R_{25}) is evaporated/stripped much earlier than expected by the classical ram pressure criterion (Gunn & Gott 1972). The key ingredient for this argument is the two-phase nature of the atomic hydrogen. In the inner disk ($R < R_{25}$) cold and warm HI coexist, whereas in the outer disk the atomic gas is mostly warm (Braun 1997). The cold HI is located near star forming regions and might be stirred by supernova explosions. This dynamical stirring causes a tangled magnetic field in the dense cold HI clouds which inhibits their evaporation by the hot intracluster medium once they are pushed out of the galactic disk by ram pressure. We further argue that the warm diffuse HI is evaporated and stripped rapidly with an evaporation rate between 10 and 100 $M_{\odot}\text{yr}^{-1}$. After a ram pressure stripping event we therefore can only observe the fraction of the ISM which was in form of dense cold clouds before it was removed from the galactic disk. More observations are needed to test our scenario of the stripping of a two-phase atomic hydrogen.

Acknowledgements. Based on observations with the 100-m telescope of the MPIfR (Max-Planck-Institut für Radioastronomie) at Effelsberg.

References

- Bothun G., Schommer R.A., Sullivan W.T.III 1982, AJ, 87, 731
- Braun R. 1997, ApJ, 484, 637
- Cayatte V., van Gorkom J.H., Balkowski C., Kotanyi C. 1990, AJ, 100, 604
- Cayatte V., Kotanyi C., Balkowski C., van Gorkom J.H. 1994, AJ, 107, 1003
- Chamaraux P., Balkowski C., Gérard E. 1980, A&A, 83, 38
- Combes, F., Dupraz, C., Casoli, F., & Pagani, L. 1988, A&A, 203, L9
- Cowie, L.L., & McKee, C.F. 1977, ApJ, 211, 135
- Cowie, L.L., McKee, C.F., & Ostriker J.P. 1981, ApJ, 247, 908
- Crowl H.H., Kenney J.P.D., van Gorkom J.H. & Vollmer B. 2005, AJ, 130, 65
- Dressler A. 2004, in: Clusters of Galaxies: Probes of Cosmological Structure and Galaxy Evolution, ed. J.S. Mulchaey, A. Dressler, & A. Oemler (New York: Cambridge Univ. Press), 207
- Elmegreen B.G. & Falgarone E. 1996 ApJ, 471, 816
- Fujita Y. 2004, PASJ, 56 29
- Gavazzi G. 1987 ApJ, 320, 96
- Gavazzi G. 1989 ApJ, 346, 59
- Gavazzi G. & Boselli A. 2006, PASP, 118, 517
- Giovanelli R., Haynes M.P. 1985, ApJ, 292, 404
- Gunn J.E., Gott J.R. 1972, ApJ, 176, 1
- Hibbard, J.E., van Gorkom, J.H., Rupen, M.P., & Schiminovich D. 2001, in: ASP Conference Series Vol. 240, "Gas and Galaxy Evolution", eds. J.E. Hibbard, J.H. van Gorkom, M.P. Rupen, p.659
- Kenney J.P.D. & Koopmann R.A. 1999, AJ, 117, 181
- Kenney J.P.D., van Gorkom J., & Vollmer B. 2004, AJ, 127, 3361
- Kulkarni S.R. & Heiles C. 1988, in: Galactic and Extragalactic Radio Astronomy, ed. G.L. Verschurr & K.I. Kellermann (Springer, Berlin), 95
- Malyshkin L. & Kulsrud R. 2001, ApJ, 549, 402
- McKee C.F. 1995 in: The Physics of the Interstellar Medium and the
- Mihos J.C. 2004, in: Clusters of Galaxies: Probes of Cosmological Structure and Galaxy Evolution, ed. J.S. Mulchaey, A. Dressler, & A. Oemler (New York: Cambridge Univ. Press), 278
- Moore B., Katz N. Lake G. et al. 1996, Nature, 379, 613
- Moore B., Lake G., & Katz N. 1998, ApJ, 495, 139
- Nulsen P.E.J. 1982, MNRAS, 198, 1007
- Oosterloo T. & van Gorkom J.H. 2005, A&A, 437, 19
- Spitzer L. 1990 ARA&A, 28, 71
- van Gorkom J.H., Kotanyi C.G. 1985, in Proceedings of the Workshop on the Virgo Cluster, edited by O.G. Richter and B. Bingelli (ESO Garching), p. 61
- Vollmer B. & Huchtmeier W. 2003, A&A, 406, 427
- Vollmer B., Balkowski C., Cayatte V., van Driel W. & Huchtmeier W. 2004a, A&A, 419, 35
- Vollmer B., Beck R., Kenney J.P.D., & van Gorkom J.H. 2004b, AJ, 127, 3375
- Vollmer B., Reich W., Wielebinski R. 2004c, A&A, 423, 57
- Vollmer B., Braine J., Combes F. & Sofue Y. 2005, A&A, 441, 473
- Vollmer B., Soida M., Otmianowska-Mazur K. et al. 2006, A&A, 453, 883
- Warmels R.H. 1988, A&AS, 72, 19
- Yoshida M., Yagi M., Okamura S. et al. 2002, ApJ, 567, 118